^{177}Lu-AMBA Biodistribution, Radiotherapeutic Efficacy, Imaging, and Autoradiography in Prostate Cancer Models with Low GRP-R Expression

Mary Ellen Maddalena, Jaclyn Fox, Jianqing Chen, Weiwei Feng, Aldo Cagnolini, Karen E. Linder, Michael F. Tweedle, Adrian D. Nunn, and Laura E. Lantry

Ernst Felder Laboratories, Bracco Research USA Inc., Princeton, New Jersey

^{177}Lu-DO3A-CH$_2$CO-G-4-aminobenzoyl-Q-W-A-V-G-H-L-M-NH$_2$ (^{177}Lu-AMBA) is a radiolabeled bombesin derivative that is bound and internalized by cells expressing the G-protein–coupled gastrin-releasing peptide receptor (GRP-R) and is currently in phase I clinical trials. In previous radiotherapy studies with PC-3 xenografted mice, ^{177}Lu-AMBA treatment significantly increased survival and reduced tumor growth rates. The PC-3 tumor cell line has an elevated expression of GRP-Rs (2.5×10^5/cell), whereas LNCaP—a prostate cancer metastatic cell line representing the early androgen-sensitive stage of prostate cancer—and DU145—an androgen-insensitive metastatic line—express lower receptor numbers (5.9×10^3 and 1.2×10^4/cell, respectively). Because of tumor heterogeneity, the high number of receptors in the PC-3 line may not represent the clinical situation, and little definitive work on the GRP-R status of primary prostate tumors and metastases exists. We sought to evaluate the tumor binding and imaging potential of ^{177}Lu-AMBA in low GRP-R models of prostate cancer and determine how reduced expression affects ^{177}Lu-AMBA radiotherapy efficacy. **Methods:** The LNCaP and DU145 cell lines were used to determine the binding (K_d), retention, and efflux of ^{177}Lu-AMBA. Biodistribution radiotherapy, imaging, and autoradiography studies were performed in LNCaP, DU145, or PC-3 tumor–bearing male nude mice. Immunohistochemistry was used to determine the proliferative state in LNCaP and DU145 models and the vascular phenotype of LNCaP radiotherapy tumors. **Results:** ^{177}Lu-AMBA binds to GRP-R in these cell lines with high affinity (K_d of LNCaP, 0.65 ± 0.2 nM; K_d of DU145, 0.53 ± 0.1 nM). The uptake of ^{177}Lu-AMBA is at least 10-fold less in LNCaP and DU145 cell lines than it is in the PC-3 cell line. Autoradiography identifies activity concentrated in areas of viable tumor tissue, and γ-images of ^{177}Lu-AMBA identify tumors in vivo. Despite having lower uptake, ^{177}Lu-AMBA demonstrated radiotherapeutic efficacy and decreased proliferation in the LNCaP and DU145 xenografts; in the LNCaP model, ^{177}Lu-AMBA normalized the phenotype of microvasculature, reducing tumoral blood pooling. **Conclusion:** ^{177}Lu-AMBA is a single radiolabeled agent that combines targeted radiotherapy after imaging dosimetry with the potential for single-agent or multimodality therapy for prostate cancer.

Key Words: gastrin-releasing peptide; prostate cancer; radiotherapeutics; imaging; ^{177}Lu

P rostate cancer is the leading cause of cancer death in men, with an estimated 186,320 cases diagnosed and more than 28,000 deaths in the United States during 2008 (*1*).

The design of a therapeutic course for the patient with prostate cancer can be particularly difficult because of the heterogeneity of the disease. The phenotypic characteristics of metastatic prostate cancer can show a broad spectrum, even within the same patient at the same time (*2*). The development of a single radiolabeled agent that could function as both a radiotherapeutic and an imaging agent for dosimetry, with the potential as an adjunct to traditional chemotherapy, could ameliorate these difficulties and result in better management of prostate cancer.

Gastrin-releasing peptide (GRP) is a 27-amino-acid mammalian bombesin–like peptide that is normally involved in smooth muscle contraction, endocrine and exocrine secretion, feeding regulation, blood pressure, thermoregulation, and cell growth (*3*). GRP exerts its effects by binding to the G-protein–coupled, 7-transmembrane receptor GRP receptor (GRP-R; BB-2). The other mammalian bombesin–related receptor subtypes are the neuromedin B receptor (NMB-R; BB-1) and the orphan receptor BB-3 (*4*). Normal GRP-R expression is limited to the nonneuroendocrine tissues of the breast and pancreas and the neuroendocrine tissues of the gastrointestinal tract, brain, prostate, and lung (*4–6*). Expression of the receptor is not normally seen in the epithelium of the prostate, colon, or lung (*3,6*). GRP-R is ectopically expressed in many human cancers, including breast, colon, and prostate, and regulates cell proliferation, differentiation,

and morphology (7–10). Elevated GRP-R expression is not confined to invasive prostate cancer but is also present in prostatic intraepithelial neoplasia, which may be an early indicator of cancer (10). This expression pattern, along with the cellular internalization characteristic of the G-protein–coupled receptors, makes GRP-R an attractive target for both imaging and radiotherapy.

We have previously shown that ^{177}Lu-AMBA, a DO3A-chelated bombesin-related peptide agonist (DO3A-CH$_2$CO-G-4-aminobenzoyl-Q-W-A-V-G-H-L-M-NH$_2$) labeled with ^{177}Lu, has a high affinity (K$_d$, 1.02 nM) for, and is internalized by, GRP-R (11). In vivo experiments demonstrated that the compound increased survival while reducing tumor load in PC-3 tumor–bearing immunocompromised male mice (11). The radionuclide ^{177}Lu was chosen because it allows for a single agent to both give high-quality γ-images and exert therapeutic effects by medium-energy β-emissions. The short path of the β-particle has the benefit of reducing normal-tissue damage (12).

Clinically, primary prostate cancer and the metastases may be heterogeneous, demonstrating a spectrum of phenotypes from androgen-sensitive to -insensitive. For the purpose of in vivo modeling, the early stages of prostate cancer are represented by the androgen-dependent, prostate-specific antigen–secreting hormone-sensitive prostate cancer cell line LNCaP, derived from a lymph node metastasis. The PC-3 cell line, derived from a bone metastasis, is androgen-independent and is thought to represent late-stage hormone-refractory prostate cancer (HRPC) (13). A second classic HRPC cell line, DU145, is also androgen-independent and is derived from a brain metastasis.

In light of the heterogeneity in metastatic prostate cancer, we sought to measure the in vitro receptor affinity and biodistribution and the radiotherapeutic efficacy of ^{177}Lu-AMBA in the low–GRP-R-expressing xenografts of the DU145 and LNCaP cell lines. We proposed that ^{177}Lu-AMBA will be clinically efficacious as a single-agent radiotherapeutic that may be imaged to facilitate personalized dosing (dosimetry) for heterogeneous metastatic prostate cancer and be a valuable adjunct to traditional chemotherapy.

MATERIALS AND METHODS

Synthesis of AMBA and Lu-AMBA

The ligand and radioactive complex were synthesized using the methods published previously (11). Nonradioactive ^{175}Lu-AMBA was prepared as described by Cagnolini et al. (14).

Cell Culture

LNCaP and DU145 cell lines were obtained from the American Type Culture Collection (ATCC). LNCaP cells were cultured on collagen-coated flasks (BD Biosciences) in RPMI 1640 (30-2001; ATCC) supplemented with 10% heat-inactivated fetal bovine serum (35-011-CV; Mediatech, Inc.). DU145 cells were grown in tissue culture–treated flasks (Corning Life Sciences) in minimum essential medium (30-2003; ATCC) supplemented with 10% heat-inactivated fetal bovine serum. The cultures were maintained in a humidified atmosphere containing 5% CO$_2$/95% air at 37°C and routinely passed using 0.25% trypsin/ethylenediaminetetraacetic acid (45000-664; VWR).

Saturation Binding and Determination of Receptor Density

In vitro saturation binding studies were performed for PC-3, DU145, and LNCaP cells as previously published (11). Briefly, PC-3 and DU145 cells were used at a density of approximately 3.0 × 10^4 cells per well in 96-well plates (Optilux-I; BD Biosciences). Because of their loosely adherent nature, LNCaP in vitro studies were run as suspension assays at a density of 5 × 10^4 cells per sample. The cells were incubated for 1 h with 55 kBq (1.5 μCi) of ^{177}Lu-AMBA containing ^{175}Lu-AMBA at concentrations between 0 and 20 nM. Parallel experiments were done with various concentrations of ^{177}Lu-AMBA in the presence of a large excess of ^{175}Lu-AMBA (1 μM) to determine nonspecific binding. Total radioactivity bound to the cells was counted (Wallac 1282; PerkinElmer). The bound counts per minute were converted to bound femtomoles based on the specific activity of the ^{177}Lu-AMBA. The maximum number of binding sites (B$_{max}$) was calculated as bound femtomoles per million cells. The receptor numbers were calculated based on the bound ligand and cell number.

Internalization and Efflux

Internalization and efflux studies were conducted for PC-3, DU145, and LNCaP cell lines as previously published (11). Briefly, PC-3 and DU145 cells were used at a density of 2.5–3.0 × 10^4 cells per well in 96-well plates. The cells were incubated with ^{177}Lu-AMBA (~118 GBq/μmol; 27.75 kBq/mL [0.75 μCi/mL]) for 40 min at 37°C, in triplicate. The wells were washed and then incubated at 4°C for 4 min with 0.2 M acetic acid. The acid wash was collected and counted to determine surface-bound radioactivity. The cells were then washed with buffer and lysed with 0.5N NaOH. The lysates were counted to determine the fraction internalized. To evaluate compound efflux, the cells were incubated with ^{177}Lu-AMBA in buffer for 40 min at 37°C, washed with 0.2 M acetic acid, and then incubated for 2 h in fresh buffer. The culture supernatants were collected and counted (Wallac 1282). LNCaP cells were studied in a suspension at a density of 1 × 10^6 cells; after the addition of ^{177}Lu-AMBA (~118 GBq/μmol; 37 kBq/mL [1.0 μCi/mL]), the cells were incubated at 37°C for 1 h, in triplicate, then washed with ice-cold binding buffer and centrifuged at 200g for 4 min at 4°C. The cells were resuspended in fresh buffer, and the incubation continued at 37°C. Activity was measured at 0, 1, and 3 h. The efflux was determined by centrifuging and counting the supernatant. The membrane-bound fraction was determined by incubating the cells on ice with 0.2 M acetic acid in saline for 4 min, centrifuging, and counting the supernatant. The internalized activity was determined by counting the remaining cell pellet.

Xenografts

All animal studies were conducted in accordance with approved Institutional Animal Care and Use Committee protocols. The subjects were 4- to 5-wk-old Tac:Cr:(NCr)-Foxn1 *nu/nu* homozygous male athymic nude mice (Taconic Farms Inc.) xenografted with human LNCaP or DU145 cells (5 × 10^6/mouse) in 0.1 mL of phosphate-buffered saline/Matrigel 1:1 (BD Biosciences) by subcutaneous injection to the right flank. The mice were housed in a high-efficiency particulate air (HEPA)–filtered environment, in

sterile HEPA-filtered cages with sterilized bedding. Sterile irradiated rodent chow and sterile filtered water, pH 2.5, were provided ad libitum. Cage changes occurred twice per week and were done in a HEPA-filtered hood. The barrier environment was maintained for the duration of the studies.

Biodistribution

Biodistributions (1 and 24 h) were performed in DU145 and LNCaP tumor–bearing mice. Mice were weighed to the nearest 0.1 g, and the weight was recorded. The average tumor sizes were 594 and 485 mg for the DU145 and the LNCaP tumor–bearing mice, respectively. Each mouse was injected with a trace dose of ^{177}Lu-AMBA (0.185 MBq/0.1 mL, ~118.4 GBq/μmol; peptide mass, 0.32 μg/m^2) via the lateral tail vein. The mice were observed at various intervals after administration, and any abnormal activity or symptoms were recorded. Food and water were provided ad libitum for the mice in the 24-h time group. The mice were sacrificed by cervical dislocation, and designated tissues and organs were harvested. Each tissue or organ and a blood aliquot were weighed to the nearest milligram and recorded, then assayed for residual radioactivity in a γ-counter (Wizard 1480; Wallac) and compared with a 100% standard. The material weights and associated counts per minute were used for the calculation of percentage injected dose (%ID) per organ and per gram of tissue (%ID/g).

Radiotherapy

The mice were identification-transpondered (IPTT-200; Bio-Medic Data Systems) subcutaneously under ketamine and xylazine anesthesia, and the incisions were sealed with Tissumend II (Veterinary Products Laboratories). After 2–3 d, the mice were xenografted as outlined above.

For the DU145 therapy, animals with tumors between 61 and 310 mm^3 were included in the study, with an average tumor size of 152 mm^3. The LNCaP radiotherapy mouse tumors averaged 124 mm^3, with a range of 53–202 mm^3. The mice for both studies ($n = 12$ per study) were administered 27.75 MBq (1.11 GBq/μmol) of ^{177}Lu-AMBA in a volume of 0.1 mL of radioprotective buffer comprising a 9:1 (v/v) mixture of bacteriostatic 0.9% sodium chloride injection (United States Pharmacopeia [USP]) and ASCOR L500 (Ascorbic Acid Injection, USP) subcutaneously to the interscapular space under sterile conditions. The peptide mass of ^{177}Lu-AMBA for the LNCaP and DU145 radiotherapeutic studies was 108.3 μg/m^2 (0.867 μg; 0.52 nmol) and 118 μg/m^2 (0.945 μg; 0.56 nmol), respectively. Previous studies from this laboratory have shown that subcutaneous and intravenous injections of ^{177}Lu-AMBA yield similar binding and retention profiles (data not shown).

The control group ($n = 12$ for each study) received vehicle only by interscapular subcutaneous injection. Observations, body weights, and tumor measurements (DAS-OAP electronic calipers; BioMedic Data Systems) were taken 3 times per week under sterile conditions. Tumor volumes were calculated by the formula $V = 1/2 L \times W^2$ (where L is a major axis and W is an orthogonal axis). Following standard animal-use protocols, termination was mandated on reaching one or both of the following criteria: a tumor weight of greater than 2 g (2-mL volume) or total body weight loss of greater than 20%. At the end of the study, or at sacrifice, tumors were harvested and snap-frozen in Tissue-Tek optimal-cutting temperature compound (Sakura Finetek USA, Inc.) by immersion in dry ice–cooled isopentane. The frozen blocks were stored at −80°C for histologic analysis.

γ-Imaging

Mice were xenografted with LNCaP, DU145, or PC-3 cells (positive control) as described above. After 4–6 wk of tumor growth, the mice were injected via the lateral tail vein with ^{177}Lu-AMBA (27.75 MBq/0.1 mL; peptide mass, ~120 μg/m^2; comparable to the preparation for radiotherapy). After 24 h, the mice were anesthetized with ketamine and xylazine, and planar images (with standards) were acquired on the Biospace Measures γ-imager fitted with a 20 mm/1.54/0.6 parallel collimator (Biospace Measures); the tumors were excised and weighed. Tumor regions of interest were analyzed for radioactivity.

Autoradiography

Twenty-micron sections of the frozen tumors were cut on a cryostat and mounted on polylysine-coated slides. After they dried, the slides were placed into autoradiography film cassettes and exposed to autoradiography film (Kodak Bio-Max MS) at room temperature for the prescribed exposure time, then developed using an M35AX-OMAT processor (Kodak). The sections were fixed in ice-cold acetone and stained with hematoxylin (MHS-16; Sigma-Aldrich) and eosin (HT110216; Sigma-Aldrich) (H&E). The H&E slides were examined with a Nikon Eclipse E800 microscope fitted with a Nikon digital DXM1200 camera and Nikon ACT-1 2.2 software. The exposed autoradiography film was scanned with an Epson Perfection V700 photo scanner and imported into Photoshop CS 8.0 for H&E photo overlay.

Histopathology and Immunohistochemistry

Tumor tissues were cryosectioned (10 μm), and serial sections were evaluated by H&E and immunohistochemistry or immuno-fluorescence staining. To reduce nonspecific binding to any mouse tissue on the sections, a bridging kit was used (PK2200, Vector M.O.M. Peroxidase kit; Vector Labs). For DU145 and PC-3 control sections, immunohistochemistry was performed with a primary antivimentin monoclonal antibody marker for cells of human mesenchymal origin (M0725 Clone V9; no cross-reactivity with mouse vimentin) (DakoCytomation) at 1:50 dilution, followed by biotinylated antimouse IgG (PK2200; Vector Labs). The marker was visualized with streptavidin-horseradish peroxidase/romulin AEC chromogen (RAEC810 L; BioCare Medical). Mouse IgG primary antibody was used on serial sections as a negative control. To confirm the human origin of the LNCaP tumors (which do not express vimentin), immunohistochemistry was performed with a rabbit polyclonal antibody to human prostate-specific antigen (GTX72905; GeneTex Inc.) at 1:50 dilution. Visualization was achieved with an immunoperoxidase system (PK6101, Vectastain Elite ABC kit, rabbit IgG; Vector Labs) and romulin AEC chromogen. Positive controls were frozen sections of human prostate carcinoma (Biochain). To establish the growing fraction of the tumors, immunohistochemistry for the nuclear proliferation marker Ki67 was performed using a rabbit polyclonal antibody (ab833; no cross-reactivity with mouse) (Abcam Inc.) at 1:25 dilution, visualized with the immunoperoxidase system and 3,3′-diaminobenzidine (DAB) substrate (SK4105, ImmPACT DAB and H-2200 DAB–enhancing solution; Vector Labs), and then counterstained. Positive controls were human breast carcinoma frozen sections (Biochain). The immunohistochemistry slides were graded in a range from completely negative to intense as described elsewhere (15). Photographs of the H&E-and immunohistochemistry-stained sections were taken as described above.

The average blood-pool area in LNCaP tumors was determined from the H&E slides by visually dividing the total area for each tumor into quadrants and scoring the percentage area comprising the blood pool in each quadrant. The percentage areas were added together and then divided by 4 to obtain the average for each tumor.

Dual staining of LNCaP radiotherapy tumors for vascular endothelial growth factor receptor-2 (VEGFR-2) and CD31 by immunofluorescence was performed on serial sections (10 μm) with a 2-stage block (BS966, Background Sniper [Biocare Medical]; X0590, Biotin Blocking System [Dako]), followed by a 2-h incubation at room temperature with a primary antibody cocktail comprising biotinylated rat antimouse CD31 (553371, BD Pharmingen) at 1:150 dilution and rabbit anti-KDR (T014; Southwestern University) at 1:10 dilution in 10% normal horse serum/1% bovine serum albumin (BSA)/0.1% polysorbate-20/phosphate-buffered saline. A secondary antibody cocktail of Qdot 655 goat antirabbit (Q11421MP; Invitrogen) at 1:100 dilution and streptavidin alexafluor 488 (S11223; Invitrogen) at 1:2,000 dilution in 1% normal horse serum/1% BSA/Tris-buffered saline (TBS) was applied and incubated for 1 h at room temperature after washing. The slides were then washed with 0.5% BSA/TBS, fixed in ice-cold acetone, and rewashed in TBS. In a dark room, the slides were coverslipped using VectaShield with 4′-6-diamidino-2-phenylindole (H-1200; Vector Labs) and visualized as described above for immunohistochemistry, using epifluorescence.

Statistical Analysis

Nonlinear regression analysis was performed on in vitro binding data (GraphPad Prism 3.0 software; GraphPad Software, Inc.). All mean values are given as ±SD. Statistical analysis of biodistribution studies used the unpaired t test; survival study analyses were done with the Kaplan–Meier analysis and log-rank tests (online GraphPad Quick Calc; Graph Pad Software, Inc.).

RESULTS

In Vitro Studies

Saturation binding studies in the DU145 and LNCaP cell lines show a high affinity in the nanomolar range for ^{177}Lu-AMBA, with a K_d of 0.53 ± 0.10 nM and 0.65 ± 0.20 nM, respectively. Affinity is comparable to our previously published data for PC-3, with a K_d of 1.02 nM (11); however, the cells express 20- to 40-fold fewer receptors than do PC-3 cells (408 fmol/million cells; $2.5 × 10^5$ GRP receptors per cell, $n = 6$). In DU145, the B_{max} was 19.5 fmol/million cells ($1.2 × 10^4$ GRP receptors per cell, $n = 1$), and in LNCaP the B_{max} was 9.9 fmol/million cells ($5.9 × 10^3$ GRP receptors per cell, $n = 3$).

The degree of internalization of ^{177}Lu-AMBA in DU145 cells was comparable to that of PC-3 cells but was slightly lower for LNCaP cells (Table 1). Compound retention at

2 h was highest in PC-3, followed by DU145, with LNCaP cells having the highest efflux.

In Vivo Studies

The biodistribution profile for ^{177}Lu-AMBA in the low receptor models, with the exception of the tumor uptake, is similar to that for PC-3 tumor–bearing mice (11) in all organs (Table 2). The primary route of clearance was renal, and the principal dosimetric target organ was the pancreas. Previous dosimetry estimates suggested that the target organ would be the pancreas and that about 55.5 kBq (1.5 Ci) may be administered to an average patient before toxicity may occur (11).

Proof of receptor specificity has been previously addressed (11). There was no statistical difference in ^{177}Lu-AMBA binding between the LNCaP and the DU145 xenografts at either 1 or 24 h. Binding in both tumor types was statistically different from PC-3 tumor binding (LNCaP, $P = 0.0018$; DU145, $P = 0.0007$, unpaired t test). All 3 xenografts showed clearance of about 50% after 24 h. The in vivo tumor binding of ^{177}Lu-AMBA to PC-3 xenografts is significantly higher than that of either DU145 or LNCaP xenografts. These results reflect the receptor-density–dependent binding of ^{177}Lu-AMBA to metastatic prostate cancer cell lines.

In radiotherapeutic studies, tumor volume measurements revealed the growth patterns of groups treated with ^{177}Lu-AMBA to be similar to that of the controls, unlike those of treated PC-3 tumors (11), although the treated mice in the LNCaP radiotherapy study exhibited a wider range of tumor load than did controls.

The clinical evaluation of oncology therapy response includes objective evaluation of parameters that do not directly involve tumor volume measurement (16). Xenografts may become encapsulated by mouse fibroblasts and can exhibit extensive destruction of tumor tissue in response to the radiotherapy, without a significant decrease in xenograft volume. The results of the radiotherapy studies were analyzed by clinical and preclinical methods including Kaplan–Meier survival curve, mean time to progression (16), World Health Organization (WHO) criteria for tumor response modified using immunohistochemistry (11), and fractional survival.

Treatment with ^{177}Lu-AMBA did not significantly increase survival in LNCaP or DU145 xenografted mice over controls (Fig. 1), although one third of the DU145-treated mice survived as opposed to 1 control mouse. The mean time to progression is the study day when the tumor

TABLE 1. In Vitro Internalization and Efflux of Radiolabeled GRP-R Binding Peptide ^{177}Lu-AMBA in DU145, LNCaP, and PC-3 Cells

Cell line	Internalized 2 h (% ± SD)	Membrane-bound 2 h (% ± SD)	Efflux 2 h (% ± SD)
DU145 ($n = 5$)	63.9 ± 6.9	16.4 ± 3.4	14.21 ± 6.9
LNCaP ($n = 5$)	47.9 ± 5.3	19.6 ± 3.3	31.38 ± 6.9
PC-3 ($n = 3$)	74.7 ± 15.3	15.3 ± 2.3	2.89 ± 1.8

TABLE 2. Biodistribution of ^{177}Lu-AMBA (0.185 MBq) in LNCaP, DU145, and PC-3 Tumor–Bearing Mice						
	1 h after dose			24 h after dose		
Organ	LNCaP ($n = 6$)	DU145 ($n = 8$)	PC-3* ($n = 9$)	LNCaP ($n = 6$)	DU145 $n = 8$	PC-3* ($n = 9$)
Tumor (%ID/g)	1.52 ± 0.94	0.95 ± 0.23	6.35 ± 2.23	0.83 ± 0.18	0.52 ± 0.22	3.39 ± 0.85
Blood (%ID/g)	0.16 ± 0.08	0.20 ± 0.06	0.46 ± 0.20	0.01 ± 0.01	0.01 ± 0.01	0.03 ± 0.02
Liver (%ID/organ)	0.21 ± 0.09	0.24 ± 0.10	0.25 ± 0.08	0.07 ± 0.03	0.08 ± 0.03	0.21 ± 0.36
Kidneys (%ID/organ)	2.84 ± 0.07	4.21 ± 1.80	2.95 ± 0.79	1.09 ± 0.14	0.92 ± 0.17	0.91 ± 0.25
Pancreas (%ID/organ)	14.65 ± 3.07	17.14 ± 2.54	17.78 ± 4.07	11.86 ± 2.83	12.41 ± 2.05	12.28 ± 3.50
Gastrointestinal (%ID/organ)	15.19 ± 2.62	10.91 ± 1.45	11.22 ± 3.29	7.21 ± 0.48	5.17 ± 0.86	5.77 ± 1.79
Skin (%ID/g)	0.30 ± 0.12	0.46 ± 0.27	0.33 ± 0.13	0.08 ± 0.02	0.07 ± 0.02	0.10 ± 0.02
Muscle (%ID/g)	0.08 ± 0.04	0.10 ± 0.03	0.09 ± 0.02	0.02 ± 0	0.01 ± 0.01	0.03 ± 0.02
Bladder/urine (%ID/organ)	62.00 ± 2.00	44.3 ± 10.38	55.66 ± 7.28	NA	NA	NA

*Data presented are from Lantry et al. (11).
NA = not applicable.

diameter (2r; r = [length × width]/2) has increased by 20% in half the animals. Treatment with ^{177}Lu-AMBA increased the mean time to progression 2-fold in LNCaP tumor–bearing mice, comparable to previously published radiotherapy data with PC-3 tumor–bearing mice (11). The DU145-treated group produced a 1.6-fold increase over controls (Table 3). In the DU145 radiotherapy group, treatment with ^{177}Lu-AMBA resulted in a reduction of progressive disease and an increase in partial recoveries but no complete tumor remissions over controls (Table 4). The LNCaP radiotherapy treatment with ^{177}Lu-AMBA resulted in an equal reduction of progressive disease and fewer partial recoveries. However, complete remission of the

LNCaP tumors was seen in 50% of the ^{177}Lu-AMBA–treated group. Previously published ^{177}Lu-AMBA radiotherapy data on PC-3 xenografts (11) showed a large reduction in progressive disease in treated mice, moderate partial response, and 31% complete tumor remissions.

The combined data show that ^{177}Lu-AMBA has therapeutic potential in prostate cancer tumor models at both high and low GRP-R expression levels and may be indicative of the potential of ^{177}Lu-AMBA as a therapeutic agent in heterogeneous prostate cancer.

Clinical Observations

The LNCaP tumor characteristically exhibits extravasation of blood (ecchymosis), which results in blue, purple, or red patches across the tumor surface. Over time, this blood pool seeps into the tumor surround and extends into the ipsilateral hind limb. There was no observable compromise in mobility. Treatment with ^{177}Lu-AMBA significantly decreased the occurrence of ecchymosis in LNCaP tumors over controls (Fig. 2). No unusual clinical events were observed in the DU145 radiotherapy group.

γ-Imaging

The 24-h γ-images of the animals demonstrated uptake of ^{177}Lu-AMBA by all of the xenografts (Supplemental Fig. 1; supplemental materials are available online only at
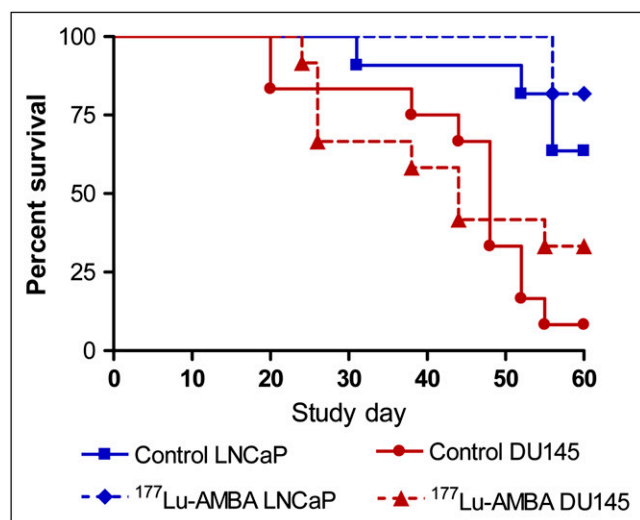

FIGURE 1. Kaplan–Meier survival curve of control vs. ^{177}Lu-AMBA-treated mice bearing LNCaP or DU145 xenografts. Each radiotherapy study consisted of control group that received vehicle alone and treated group that received ^{177}Lu-AMBA (27.75 MBq). Within each tumor type, there was no significant difference in fractional survival between control and treated groups. Control LNCaP mice vs. treated LNCaP mice: $P = 0.529$; control DU145 mice vs. treated DU145 mice: $P = 0.484$ (log-rank test).

TABLE 3. Tumor Mean Time to Progression After ^{177}Lu-AMBA Treatment (27.75 MBq) in LNCaP and DU145 Tumor–Bearing Mice, Compared with PC-3 Historic Data	
Group	Mean time to progression (d)
LNCaP control	14
LNCaP + ^{177}Lu-AMBA	28
DU145 control	7
DU145 + ^{177}Lu-AMBA	11
PC-3 control*	19
PC-3 + ^{177}Lu-AMBA*	37

*Data presented are from Lantry et al (11).

TABLE 4. Modified WHO 2-Dimensional Criteria as Applied to DU145, LNCaP, and PC-3 Radiotherapies

	PC-3* (120 d)		LNCaP (60 d)		DU145 (60 d)	
Classification	Control	Treated	Control	Treated	Control	Treated
Progressive disease	100%	22%	91%	42%	92%	42%
Stable disease	0	3%	0	0	0	0
Partial response	0	44%	9%	8%	8%	58%
Complete response	0	31%	0	50%	0	0

*Data presented are from Lantry et al. (11).

http://jnm.snmjournals.org). As seen in Table 5, the calculated %ID reflects the relative difference in receptor numbers (Table 1), with PC-3 tumor uptake and retention of radioligand about 10-fold higher than either DU145 or LNCaP uptake. No significant difference between DU145 and LNCaP %ID or %ID/g of tumor tissue was observed.

Autoradiography

To correlate the planar images with viable tumor cells, autoradiography was performed on sections of PC-3 and LNCaP imaged tumors and superimposed on serial H&E sections (Fig. 3). No radiolabel was seen in necrotic areas. The ^{177}Lu-AMBA was localized to areas of viable tumor tissue, indicative of cell-specific uptake. There is little accumulation of radioactivity in areas of blood pooling.

Immunohistochemistry

All of the DU145 radiotherapy tumors stained positively for vimentin, and LNCaP tumors were positive for human

FIGURE 2. Photographs of LNCaP ecchymosis. (A) Control mouse on study day 22. (B) ^{177}Lu-AMBA–treated mouse on study day 28. (C) LNCaP xenograft shows reduced ecchymosis when compared with control. Mice treated with ^{177}Lu-AMBA (27.75 MBq) had significant reduction in observable ecchymosis (P = 0.0056, log-rank test). Observations were made 3 times per week for duration of study.

prostate-specific antigen, confirming their human origin. To investigate the reduction of ecchymosis in the LNCaP ^{177}Lu-AMBA treatment group, immunofluorescence staining was performed on representative sections of LNCaP tumors from treated and control groups. VEGFR-2 staining for angiogenic vessels showed more VEGFR-2–positive vessels, which were larger and more amorphous in the control group than in the treated tumor groups. CD31 staining for mature vessels revealed that there were more CD31-positive/VEGFR2-negative vessels in the treated tumors, with more organized structure (Fig. 4).

The percentage blood-pool involvement, as a mathematic representation of the expression of ecchymosis, was compared in control versus treated LNCaP tumors. The control tumors had an average of 49% of the total area comprising the intratumoral blood pool, whereas only 17% of the total area of the treated tumors demonstrated blood pooling (Fig. 5). The PC-3 and DU145 tumor models do not present the blood-pooling phenotype. In the LNCaP radiotherapy study, on average there was more proliferation (68%), as assessed by Ki67 antibody staining (Supplemental Fig. 2), in the control tumors than in the treated tumors (35%). In comparison, the DU145 radiotherapy control tumors stained positively for Ki67 in 86% of the cell mass, as compared with 53% of the cell mass in the ^{177}Lu-AMBA–treated tumors (Supplemental Fig. 2). Histology thus confirmed the reduction of blood-pool involvement and the resultant ecchymosis after treatment with ^{177}Lu-AMBA in the LNCaP-treated tumors in addition to a decrease in

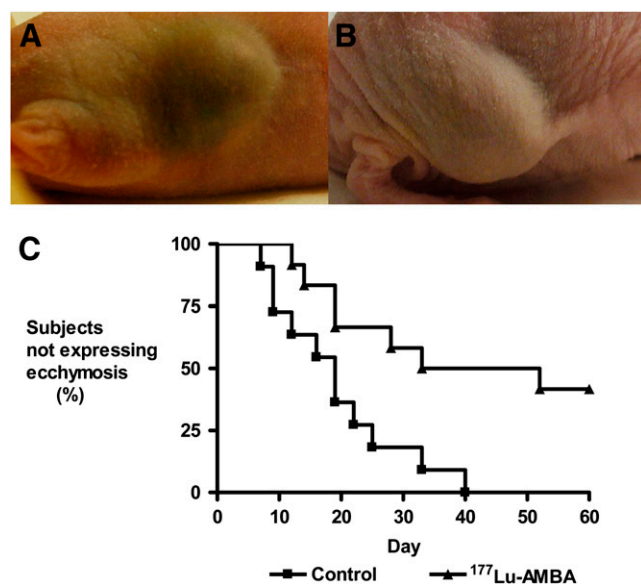**TABLE 5.** Analysis of ^{177}Lu-AMBA Tumor Uptake Calculated from Planar γ-Camera Acquisition

Cell line	Average tumor weight (g)	ROI %ID	%ID/g
PC-3 (n = 5)	0.28 ± 0.07	0.92 ± 0.31	2.70 ± 0.90
LNCaP (n = 3)	0.27 ± 0.09	0.15 ± 0.09	0.26 ± 0.13
DU145 (n = 2)	0.33 ± 0.03	0.16 ± 0.03	0.17 ± 0.04

Mice bearing PC-3, LNCaP, or DU145 tumors received intravenous injection of ^{177}Lu-AMBA (27.75 MBq). After 24-h residence, mice were anesthetized and planar images were acquired. Tumor ROI were analyzed for ^{177}Lu activity. Tumors were then excised, weighed, and counted. ROI = region of interest.
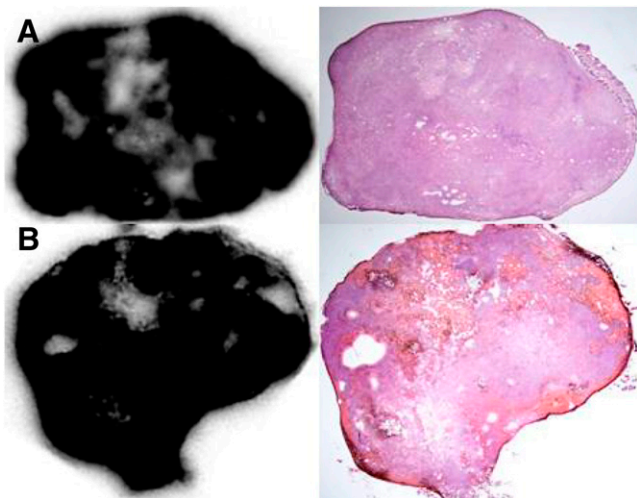
FIGURE 3. Representative autoradiographs (left) and H&E staining (right) of imaged PC-3 (row A) and LNCaP (row B) xenografts. PC-3 tumor sections were exposed to film for 6 h, LNCaP sections for 24 h.

proliferation and the reduction in proliferative cells in the DU145 ^{177}Lu-AMBA–treated tumors as reflected in the survival curves (Fig. 1).

DISCUSSION

This report demonstrates that ^{177}Lu-AMBA is a single radiolabeled agent that combines targeted radiotherapy after imaging dosimetry and has therapeutic potential in models of low–GRP-R-expressing prostate cancer representative of early-stage heterogeneous prostate cancer, complementing our previously published work with the PC-3 model of more advanced HRPC. ^{177}Lu-AMBA binds to GRP-R in the models tested here with high affinity (<1 nM) and the resultant internalization and retention of therapeutic dose levels of ^{177}Lu-AMBA results in clear labeling of LNCaP and DU145 tumors. The corresponding autoradiography of LNCaP and PC-3 xenografts support
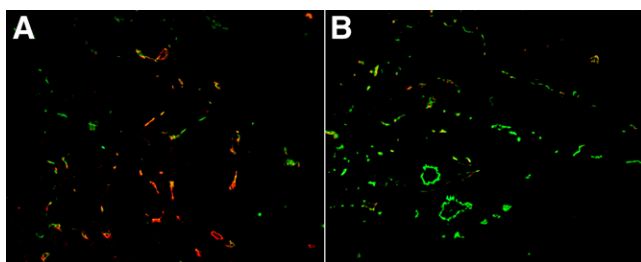

FIGURE 4. Representative histomicrographs of LNCaP from control mice and ^{177}Lu-AMBA-treated mice. Control LNCaP tumors (A) show greater population of amorphous VEGFR-2 (red) immunofluorescent staining vessels than do treated LNCaP tumors (B). Treated tumors show increase of CD31-positive (green) organized vessels. Areas of overlapping VEGFR-2 and CD31 immunoreactivity are present (yellow) in both specimens. (×10)
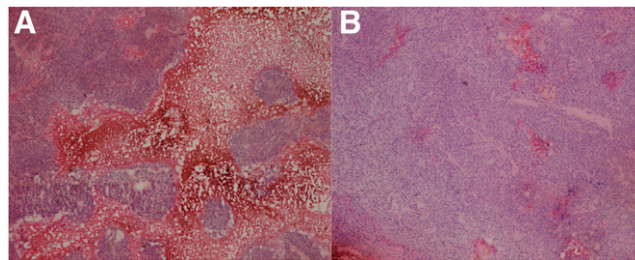

FIGURE 5. Representative histomicrographs show that relative area of blood pooling in LNCaP tumors was higher in control LNCaP tumors (A) than in treated tumors (B). (×40)

cell-specific uptake of ^{177}Lu-AMBA. Although ^{177}Lu is not the optimal radionuclide for imaging outside the context of an imaging/radiotherapy pair, it has already been demonstrated that gallium-AMBA behaves biologically like lutetium-AMBA (*17*) and that, clinically, ^{68}Ga-AMBA provides good images of prostate and breast cancer (*18*).

The statistics generated by this planned short-term (60 d) survival study do not support an increase in survival fraction, although in our previous studies with PC-3 xenografts we gave more than 1 dose, followed the animals for longer, and demonstrated an increase in survival (*11*). However, the extension of the tumor mean time to progression, increase in WHO criteria partial response in the DU145 tumor model, emergence of complete remission in the LNCaP study, and reduction of LNCaP ecchymosis are all indications of beneficial effects from treatment with ^{177}Lu-AMBA.

Ecchymosis results from a leaky, defective tumor vasculature. Tumor vessels that are haphazardly arranged and lack a discernible hierarchy of arterioles, capillaries, and venules are a hallmark of solid tumors (*19,20*). In addition, abnormal endothelial cell and pericyte structure and function can result in a defective basement membrane and instability of the vessel walls, causing hemorrhage (*19,21*). Blood pooling from extravasated red blood cells was evident from our histology of LNCaP xenografts. This blood pooling, coupled with high intratumoral pressures resulting from mechanical stress and lack of adequate lymphatic drainage, results in a reduced transmural gradient that is an impediment to intravenously administered therapies (*21,22*). Here, treatment with ^{177}Lu-AMBA appeared to alter the vascular permeability of the LNCaP xenografts, resulting in the clinically observed reduction in ecchymosis and histologically verified reduction in blood pooling.

The normalization of the vasculature could be a direct effect of ^{177}Lu-AMBA β-emissions on endothelial cells. Previous in vitro autoradiography studies with ^{177}Lu-AMBA in human cancers have shown GRP-R–positive peritumoral vessel binding (*23*). Endothelial cells of the tumor vasculature appear to have high mitotic and apoptotic rates, which would contribute to radiosensitivity (*24,25*). There is evidence that the tumor vessel lining can comprise a mixture of tumor, pericyte, endothelial, and stromal cells;

perhaps each cell type makes a contribution to radiosensitivity. Studies in acid sphingomyelinase-deficient and wild-type mice have shown that ionizing radiation at clinical dose levels causes endothelial cell apoptosis, which in turn regulates tumor cell response (26). Our immunofluorescent antibody data suggest that LNCaP tumors treated with ^{177}Lu-AMBA have an increase in mature, organized, CD31-staining vessels when compared with controls, which exhibit a greater population of amorphic, angiogenic VEGFR-2–positive vessels. We propose that the ^{177}Lu-AMBA dose internalized by LNCaP tumors is sufficient to reduce permeability of the vasculature and create a more normal phenotype of microvessels and may, therefore, provide a more efficient route for further treatment. Recently, antiangiogenic therapy studies using anti-VEGF antibodies have shown normalization of tumor vessel structure, including a reduction in vascular permeability and restored transvascular pressure gradients and demonstrating improved perfusion of therapeutic agents (27,28). The exact mechanism for this normalization in LNCaP tumors would require further study.

Our observed reduction in proliferation in both the LNCaP and the DU145 cell lines shows that the internalized dose of ^{177}Lu-AMBA is sufficient to cause tumor cell death or senescence. One of the benefits of a ^{177}Lu-labeled therapeutic is the relatively long half-life (6.7 d), prolonging the residence time in the tumor and increasing the chance for therapeutic effect. Comet assay of genomic DNA has shown that both DU145 and LNCaP cells suffer significant levels of DNA damage when exposed to ionizing radiation treatment (29). This is supported by our Ki67 and 4′-6-diamidino-2-phenylindole staining, showing reduced cell mass or proliferation in both types of xenografts after treatment with ^{177}Lu-AMBA.

CONCLUSION

The internalized dose of ^{177}Lu-AMBA, even in the low–GRP-R-expressing models of prostate cancer—LNCaP and DU145—is sufficient to reduce cell proliferation and tumor growth rate. In addition to being a single-agent radiotherapeutic that combines targeted radiotherapy after imaging dosimetry, the normalized tumor vessels in the treated LNCaP xenografts suggest ^{177}Lu-AMBA radiotherapy may serve as a possible adjunct to intravenously administered chemotherapy.

REFERENCES

1. American Cancer Society. *Cancer Facts and Figures 2008*. Atlanta, GA: American Cancer Society; 2008.
2. Shah RB, Mehra R, Chinnaiyan AM, et al. Androgen-independent prostate cancer is a heterogeneous group of diseases: lessons from a rapid autopsy program. *Cancer Res.* 2004;64:9209–9216.
3. Ohki-Hamazaki H, Iwabuchi M, Maekawa F. Development and function of bombesin-like peptides and their receptors. *Int J Dev Biol.* 2005;49:293–300.
4. Woodruff GN, Hall MD, Reynolds T, Pinnock RD. Bombesin receptors in the brain. *Ann N Y Acad Sci.* 1996;780:223–243.
5. Sunday ME. Tissue-specific expression of the mammalian bombesin gene. *Ann N Y Acad Sci.* 1988;547:95–113.
6. Nagy A, Schally AV. Targeting cytotoxic conjugates of somatostatin, luteinizing hormone-releasing hormone and bombesin to cancers expressing their receptors: a "smarter" chemotherapy. *Curr Pharm Des.* 2005;11:1167–1180.
7. Reubi JC. Peptide receptors as molecular targets for cancer diagnosis and therapy. *Endocr Rev.* 2003;24:389–427.
8. Scopinaro F, De Vincentis G, Corazziari E, et al. Detection of colon cancer with [99mTc]-labeled bombesin derivative ([99mTc]-Leu13-BN1). *Cancer Biother Radiopharm.* 2004;19:245–252.
9. Reile H, Armatis PE, Schally AV. Characterization of high-affinity receptors for bombesin/gastrin releasing peptide (GRP) on the human prostate cancer cell lines PC3 and DU145; internalization of receptor bound [125]I-[Tyr⁴] bombesin by tumor cells. *Prostate.* 1994;25:29–38.
10. Markwalder R, Reubi JC. Gastrin-releasing peptide receptors in the human prostate; relation to neoplastic transformation. *Cancer Res.* 1999;59:1152–1159.
11. Lantry LE, Cappelletti E, Maddalena ME, et al. ^{177}Lu-AMBA: Synthesis and characterization of a selective ^{177}Lu-labeled GRP-R agonist for systemic radiotherapy of prostate cancer. *J Nucl Med.* 2006;47:1144–1152.
12. Panigone S, Nunn AD. Lutetium-177-labeled gastrin releasing peptide receptor binding analogs: a novel approach to radionuclide therapy. *Q J Nucl Med Mol Imaging.* 2006;50:310–321.
13. Navone NM, Logothetis CJ, von Eschenbach AC, Troncoso P. Model systems of prostate cancer: uses and limitations. *Cancer Metastasis Rev.* 1998–1999;17: 361–371.
14. Cagnolini A, D'Amelio N, Metcalfe E, et al. Isolation of a [177]Hf complex formed by β-decay of a ^{177}Lu-labeled radiotherapeutic compound, and NMR structural elucidation of the ligand and its Lu and Hf complexes. *Inorg Chem.* 2009;48: 3114–3124.
15. Han Z, Slack RS, Wenping L, Papadopoulos V. Expression of peripheral benzodiazepine receptor (PBR) in human tumors: relationship to breast, colorectal, and prostate tumor progression. *J Receptor and Sig Trans Res.* 2003;23: 225–238.
16. Therasse P, Arbuck S, Eisenhauer EA. New guidelines to evaluate the response to treatment in solid tumors. *J Natl Cancer Inst.* 2000;92:205–216.
17. Fox J, Maddalena M, Wedeking J, et al. Comparative biodistributions of ^{111}In, ^{67}Ga and ^{177}Lu-AMBA in PC-3 tumor bearing mice [abstract]. *J Nucl Med.* 2007;48(suppl 2):79P.
18. Baum RP, Prasad V, Mutloka N, et al. Molecular imaging of bombesin receptors in various tumors by Ga-68 AMBA PET/CT: first results [abstract]. *J Nucl Med.* 2007;48(suppl 2):79P.
19. Jain RK. Molecular regulation of vessel maturation. *Nat Med.* 2003;9:685–693.
20. McDonald DM, Baluk P. Significance of blood vessel leakiness in cancer. *Cancer Res.* 2002;62:5381–5385.
21. Fukumura D, Jain RK. Tumor microenvironment abnormalities: causes, consequences, and strategies to normalize. *J Cell Biochem.* 2007;101:937–949.
22. Baluk P, Hashizume H, McDonald DM. Cellular abnormalities of blood vessels as targets in cancer. *Curr Opin Genet Dev.* 2005;15:102–111.
23. Waser B, Eltschinger V, Linder K, et al. Selective in vitro targeting of GRP and NMB receptors in human tumours with the new bombesin tracer ^{177}Lu-AMBA. *Eur J Nucl Med Mol Imaging.* 2007;34:95–100.
24. Denekamp J. Vascular attack as a therapeutic strategy for cancer. *Cancer Met Rev.* 1990;9:267–282.
25. Hashizume H, Baluk P, Shunichi M. Openings between defective endothelial cells explain tumor vessel leakiness. *Am J Pathol.* 2000;156:1363–1380.
26. Garcia-Barros M, Paris F, Cordon-Cardo C, et al. Tumor response to radiotherapy regulated by endothelial cell apoptosis. *Science.* 2003;300:1155–1159.
27. Tong RT, Boucher Y, Kozin SV, et al. Vascular normalization by vascular endothelial growth factor receptor 2 blockade induces a pressure gradient across the vasculature and improves drug penetration in tumors. *Cancer Res.* 2004;64: 3731–3736.
28. Wildiers H, Guetens G, De Boeck G, et al. Effect of antivascular endothelial growth factor treatment on the intratumoral uptake of CPT-11. *Br J Cancer.* 2003;88:1979–1986.
29. Cardile V, Bellia M, Lombardo L, et al. Distinct response to ionizing radiation of human prostate cell lines. *Oncol Rep.* 2005;14:981–985.